Rapidity dependence of jet shape broadening and quenching

I. P. Lokhtin, S. V. Petrushanko, L. I. Sarycheva, and A. M. Snigirev

M.V. Lomonosov Moscow State University, D.V. Skobeltsyn Institute of Nuclear Physics, Ru-119992 Leninskie Gory, Moscow, Russia

The jet shape modification due to partonic energy loss in the dense QCD matter is investigated with the help of the special transverse energy-energy correlator in the vicinity of maximum energy deposition of every event. In the accepted scenario with scattering of jet hard partons off comoving medium constituents this correlator is independent of the pseudorapidity position of a jet axis and becomes considerably broader (symmetrically over the pseudorapidity and the azimuthal angle) in comparison with *pp*-collisions. At scattering off "slow" medium constituents the broadening of correlation functions is dependent on the pseudorapidity position of a jet axis and increases noticeably in comparison with the previous scenario for jets with large enough pseudorapidities. These two considered scenarios result also in the different dependence of jet quenching on the pseudorapidity.

PACS number(s): 25.75.−q, 12.38.Mh, 24.85.+p

I. INTRODUCTION

Experimental results from the CERN Super Proton Synchrotron (SPS) have revealed a rich set of new phenomena as the anomalous suppression of charmonium [1] and the broadening or mass shift of vector mesons [2] indicating the formation of dense matter [3,4]. However, it has proven difficult to disentangle hadron contributions to the observed signals, and no clear consensus has emerged that a long lived quark-gluon plasma (QGP) has been observed in the fixed target heavy ion experiments at those facilities. Experiments at the BNL Relativistic Heavy Ion Collider (RHIC), which began operation in 2000, have initiated a new era in the study of QCD matter under extreme conditions. Nuclear collisions at the largest RHIC energy ($\sqrt{s_{NN}} = 200$ GeV) not only produce matter at the highest energy density ever achieved but also provide a number of rare observables that have not been accessible previously. Already in the first three years of RHIC operation the wealth of new data has been collected and analyzed such as a strong elliptic flow, the suppression of hadron spectra and azimuthal back-to-back two-particle correlations indicating that a dense equilibrated system is generated in the most violent head-on collisions of heavy nuclei (see, for instance, a review [5] and references therein).

The c.m. energy for heavy ion collisions at the CERN Large Hadron Collider (LHC) ($\sqrt{s_{NN}} = 5.5$ TeV) will exceed that at RHIC by a factor of about 30. This provides exciting opportunities for addressing unique physics issues in a new energy domain, where hard and semihard QCD multiparticle production can stand out against the underlying soft events. Besides the statistics is expected to be high enough [6] for the systematic analysis of various aspects of QCD-physics (poorly accessible for studying at RHIC energy) in the medium with the initial energy density considerably above the critical one for the deconfinement transition. In particular it will be possible to study the modification of jet shape and spectra in comparison with *pp*-collisions. Jets as one of the important probes of quark-gluon plasma are created at the very beginning of the collisions process ($\tau_{\text{form}} \sim 1/p_T \lesssim 0.01$ fm/*c*) by the initial hard parton-parton scatterings. These

hard partons pass through the dense matter formed at longer time scales ($\gtrsim 0.1$ fm/*c*) and interact strongly with the medium constituents changing its original properties (the momentum direction, energy, particle distribution inside a jet) as a result of in-medium rescattering.

One of the encouraging methods for investigation of these effects seems to be the measurement of energy-energy correlations [7,8]. In the present paper we extend our approach [8], considering the energy-energy correlator in the restricted rapidity-angle space in the vicinity of maximum energy deposition of every event. This special correlator allows us to investigate, using the calorimetric information, the broadening of the jet shape due to partonic energy loss which is intensively discussed in the current literature [9].

II. ENERGY CORRELATORS IN ELECTRON-POSITRON, HADRON AND NUCLEAR COLLISIONS

To be clear at first we recall the well-known definition of the energy-energy correlation function Σ which has been used by all for LEP experiments [10] at CERN and the SLD experiment [11] at SLAC to measure the strong coupling constant α_s in e^+e^--annihilation at the Z^0 resonance with a high accuracy. Σ is defined as a function of the angle χ between two particles i and j in the following form:

$$\frac{d\Sigma(\chi)}{d\cos(\chi)} = \frac{\sigma}{\Delta\cos(\chi)N_{\text{event}}} \sum_{\text{event}} \sum_{i \neq j} \frac{E_i E_j}{E^2}, \quad (1)$$

where σ is the total cross section for $e^+e^- \rightarrow$ hadrons, E is the total energy of the event, E_i and E_j are the energies of the particles i and j. The sum runs over all pairs i, j with $\cos(\chi_{ij})$ in a bin width $\Delta\cos(\chi)$:

$$\cos(\chi) - \Delta\cos(\chi)/2 < \cos(\chi_{ij}) < \cos(\chi) + \Delta\cos(\chi)/2.$$

The limits $\Delta\cos(\chi) \rightarrow 0$ and $N_{\text{event}} \rightarrow \infty$ have to be taken in Eq. (1).

This function can be calculated in perturbative QCD as a series in α_s:

$$\frac{1}{\sigma_0}\frac{d\Sigma(\chi)}{d\cos(\chi)} = \frac{\alpha_s(\mu)}{2\pi}A(\chi) + \left(\frac{\alpha_s(\mu)}{2\pi}\right)^2$$
$$\times \left(\beta_0 \ln\left(\frac{\mu}{E}\right)A(\chi) + B(\chi)\right) + O(\alpha_s^3), \quad (2)$$

where $\beta_0 = (33 - 2n_f)/3$, n_f is the number of active flavors at the energy E, σ_0 is the Born cross section, μ is the renormalization scale. The first order term $A(\chi)$ has been calculated by Basham *et al.* [12] from the well-known one gluon emission diagrams $\gamma^*, Z^0 \rightarrow q\bar{q}g$ with the result

$$A(\chi) = C_F(1+\omega)^3\frac{1+3\omega}{4\omega}((2-6\omega^2)$$
$$\times \ln(1+1/\omega) + 6\omega - 3), \quad (3)$$

where $C_F = 4/3$, $\omega = \cot^2(\chi)/2$ and χ is the angle between any of the three partons initiating the three hadron jets. This allowed one to determine the strong coupling constant directly from a fit to the energy-energy correlations in e^+e^--annihilation, since Σ is proportional to α_s in the first order.

In hadronic and nuclear collisions jets are produced by hard scatterings of partons. In this case it is convenient to introduce the transverse energy-energy correlations which depend very weakly on the structure functions [13] and manifest directly the topology of events. Thus, for instance, in high-p_T two-jet events the correlation function is peaked at the azimuthal angle $\varphi = 0°$ and $\varphi = 180°$, while for the isotropic background this function is independent of φ.

Utilization of hard jet characteristics to investigate QGP in heavy ion collisions is complicated because of a huge multiplicity of "thermal" secondary particles in an event. Various estimations give from 1500 to 6000 charged particles per rapidity unit in a central Pb+Pb collision at LHC energy, and jets can be really reconstructed against the background of energy flux beginning from some threshold jet transverse energy $E_T^{\rm jet} \sim 50 - 100$ GeV [6,14]. The transverse energy-energy correlation function is just sensitive to the jet quenching as well as to the global structure of energy flux (i.e., its anisotropy for non-central collisions) if we select events by an appropriate way [8]. The generalization of Eq. (1) for calorimetric measurements of the energy flow is straightforward:

$$\frac{d\Sigma_T(\varphi)}{d\varphi} = \frac{1}{\Delta\varphi N_{\rm event}}\sum_{\rm event}\sum_i \frac{E_{Ti}E_{T(i+n)}}{(E_T^{\rm vis})^2}, \quad (4)$$

where

$$E_T^{\rm vis} = \sum_i E_{Ti}$$

is the total transverse energy in N calorimetric sectors covering the full azimuth, E_{Ti} is the transverse energy deposition in the sector i ($i = 1, \ldots, N$) in the considered pseudorapidity region $|\eta|$, $n = [\varphi/\Delta\varphi]$ (the integer part of the number $\varphi/\Delta\varphi$), $\Delta\varphi \sim 0.1$ is the typical azimuthal size of a calorimetric sector. In the continuous limit $\Delta\varphi \rightarrow 0$, $N = [2\pi/\Delta\varphi] \rightarrow \infty$ Eq. (4)

reads

$$\frac{d\Sigma_T(\varphi)}{d\varphi} = \frac{1}{N_{\rm event}}\sum_{\rm event}\frac{1}{(E_T^{\rm vis})^2}\int_0^{2\pi}d\phi\frac{dE_T(\phi)}{d\phi}\frac{dE_T(\phi+\varphi)}{d\phi},$$
$$(5)$$

where $E_T^{\rm vis} = \int_0^{2\pi}d\phi\frac{dE_T(\phi)}{d\phi}$, $\frac{dE_T}{d\phi}$ is the distribution of transverse energy flow over azimuthal angle ϕ.

In our previous work [8] it was shown that at the special selection of events for the analysis (at least one high-p_T jet) and the procedure of event-by-event background subtraction in high multiplicity heavy ion collisions, the transverse energy-energy correlator (4) is sensitive to the partonic energy loss and angular spectrum of radiated gluons. The medium-modified energy-energy correlation function manifests significant strengthening in a wide interval of azimuthal angles around $\pi/2$, moderate broadening of the near-side jet region $\varphi \lesssim 0.5$ and weak additional suppression of back-to-back correlations for $\varphi \sim \pi$. Without jet trigger this correlation function shows the global structure of transverse energy flux: the correlator is isotropic for central collisions and for noncentral collisions it is sensitive to the azimuthal anisotropy of energy flow reproducing its Fourier harmonics but with the coefficients squared.

Here we extend our approach [8], considering the energy-energy correlator in the restricted rapidity-angle space in the vicinity of maximum energy deposition of every event (Fig. 1). It is convenient to define this special correlator in the following form:

$$\frac{d\Sigma_T(\eta)}{d\eta} = \frac{1}{\Delta\eta N_{\rm event}}\sum_{\rm event}\sum_{kl}\frac{E_{Tk}E_{Tl}}{(E_T^{\rm vis})^2 - \sum_j E_{Tj}^2}$$
$$\times \delta(k-l-m), \quad (6)$$

where E_{Tk} is the transverse energy deposition in the pseudorapidity strip k ($k = -M, \ldots, -1, 0, +1, \ldots, +M$) with the width $\Delta\eta \sim 0.1$ and the position of a jet axis in the strip $k = 0$, summarized over all azimuthal sectors i ($i = -M, \ldots, -1, 0, +1, \ldots, +M$) with the size $\Delta\phi = \Delta\eta$ and the position of a jet axis in the angle sector $i = 0$; $m = [\eta/\Delta\eta]$ (the integer part of the number $\eta/\Delta\eta$). Here $E_T^{\rm vis} = \sum_l E_{Tl}$ is the total transverse energy deposition in the square of $\eta \times \phi$ space, the center of which is determined by the position of a jet axis. The similar definition can be written for the correlator as a function of the azimuthal angle [it is necessary to replace $\eta \leftrightarrow \phi$ in Eq. (6) only]. The autocorrelation term $\sum_l E_{Tl}^2$ is subtracted in the denominator of the definition in order
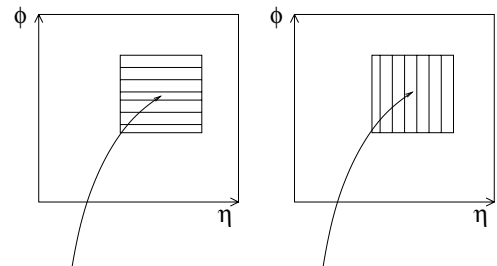

FIG. 1. The region of $\eta \times \phi$ space used in order to calculate correlators in the near-side jet region.

to normalize the integral (the sum) of correlator over η to one in the fixed square around the jet with the number of pseudorapidity strips and angle sectors $(2M + 1)$.

III. A MODEL FOR ENERGY LOSS OF A JET

We demonstrate the productivity and effectiveness of such correlators in the framework of our well worked-out model of jet passing through a medium. The model has been early applied to the calculation of various observables sensitive to the partonic energy loss: the impact parameter dependence of the jet production [15], the mono/dijet rate enhancement [16,17], the dijet rate dependence on the angular jet cone [18], the elliptic coefficient of the jet azimuthal anisotropy [19–22], the anticorrelation between the softening jet fragmentation function and the suppression of the jet rate [23]. The validity of approximations used has been verified by the comparison of RHIC data with the model calculations. The agreement is good [24] at the reasonable choice of main model parameters taking into account their dependence on the collision energy. At present the model has been constructed as the fast Monte Carlo event generator PYQUEN (PYthia QUENched), and corresponding FORTRAN routine pyquen is available via the internet [25]. The routine is implemented as a modification of the standard PYTHIA jet events [26]. For details one can refer to these mentioned papers (mainly, Refs. [15,18,23,24]). Here we note only the main steps essential for the present investigation.

The energy-energy correlator depends on not only the absolute value of partonic energy loss, but also on the angular spectrum of in-medium radiated gluons. Since coherent Landau-Pomeranchuk-Migdal radiation induces a strong dependence of the radiative energy loss of a jet on the angular cone size [18,27–30], it will soften particle energy distributions inside the jet, increase the multiplicity of secondary particles, and to a lesser degree, affect the total jet energy. On the other hand, collisional energy loss turns out to be practically independent of the jet cone size and causes the loss of total jet energy, because the bulk of "thermal" particles knocked out of the dense matter by elastic scatterings fly away in an almost transverse direction relative to the jet axis [18]. Thus although the radiative energy loss of an energetic parton dominates over the collisional loss by up to an order of magnitude, the relative contribution of the collisional loss of a jet grows with increasing jet cone size due to the essentially different angular structure of loss for two mechanisms [18]. Moreover, the total energy loss of a jet will be sensitive to the experimental capabilities to detect low-p_T particles—products of soft gluon fragmentation: thresholds for a giving signal in calorimeters, influence of the strong magnetic field, etc. [31].

Since the full treatment of the angular spectrum of emitted gluons is rather sophisticated and model-dependent [18,27–30], we considered two simple parametrizations of the distribution of in-medium radiated gluons over the emission angle θ. The "small-angular" radiation spectrum was parametrized in the form

$$\frac{dN^g}{d\theta} \propto \sin\theta \exp\left(-\frac{(\theta - \theta_0)^2}{2\theta_0^2}\right), \qquad (7)$$

where $\theta_0 \sim 5^0$ is the typical angle of the coherent gluon radiation estimated in Ref. [18]. The "broad-angular" spectrum has the form

$$\frac{dN^g}{d\theta} \propto \frac{1}{\theta}. \qquad (8)$$

We believe that such a simplified treatment here is enough to demonstrate the sensitivity of the energy-energy correlator to the medium-induced partonic energy loss.

PYTHIA_6.2 [26] was used to generate the initial jet distributions in nucleon-nucleon sub-collisions at $\sqrt{s} = 5.5$ TeV. After that, event-by-event Monte Carlo simulation of rescattering and energy loss of jet partons in QGP was performed. The approach relies on accumulative energy losses, when gluon radiation is associated with each scattering in the expanding medium together with including the interference effect by the modified radiation spectrum as a function of decreasing temperature. Such a numerical simulation of the free path of a hard jet in QGP allows any kinematical characteristic distributions of jets in the final state to be obtained. Besides, the different scenarios of medium evolution can be considered. In each ith scattering a fast parton loses energy collisionally and radiatively, $\Delta e_i = t_i/(2m_0) + \omega_i$, where the transfer momentum squared t_i is simulated according to the differential cross section for elastic scattering of a parton with energy E off the "thermal" partons with energy (or effective mass) $m_0 \sim 3T \ll E$ at temperature T, and ω_i is simulated according to the energy spectrum of coherent medium-induced gluon radiation in the Baier-Dokshitzer-Mueller-Schiff formalism [27]. Finally we suppose that in every event the energy of an initial parton decreases by the value $\Delta E = \sum_i \Delta e_i$.

The medium was treated as a boost-invariant longitudinally expanding quark-gluon fluid, and partons as being produced on a hyper-surface of equal proper times τ [32]. For certainty we used the initial conditions for the gluon-dominated plasma formation expected for central Pb+Pb collisions at LHC [33]: $\tau_0 \simeq 0.1$ fm/c, $T_0 \simeq 1$ GeV. For noncentral collisions we suggest the proportionality of the initial energy density to the ratio of the nuclear overlap function and the effective transverse area of nuclear overlapping [15].

In the frame of this model and using above QGP parameters we evaluate the mean energy loss of quark of $E_T = 100$ GeV in minimum-bias Pb+Pb collisions, $\langle \Delta E_T^q \rangle \sim 25$ GeV (accordingly, the gluon energy loss is $\langle \Delta E_T^g \rangle = 9/4$ $\langle \Delta E_T^q \rangle$). In our simulation the value of energy loss in fact is regulated mainly by the initial temperature T_0.

IV. NUMERICAL RESULTS AND DISCUSSION

To be specific, we consider the geometry of the Compact Muon Solenoid (CMS) detector [31] at LHC. The central (barrel) part of the CMS calorimetric system covers the pseudorapidity region $|\eta| < 1.5$, the segmentation of electromagnetic and hadron calorimeters being $\Delta\eta \times \Delta\phi = 0.0174 \times 0.0174$ and $\Delta\eta \times \Delta\phi = 0.0872 \times 0.0872$, respectively [31]. The endcap part of the CMS calorimeter $1.5 < |\eta| < 3$ has more tangled structure: the tower sizes of hadron calorimeter over η and ϕ are 0.087 at $|\eta| = 1.5$ and increase gradually up to 0.345 at $|\eta| = 3$.

Then the energy-energy correlation function (6) is calculated for the events containing at least one jet with $E_T^{\text{jet}} > E_T(\text{threshold}) = 100$ GeV in the considered kinematical region. The final jet energy is defined here as the total transverse energy of final particles collected around the direction of a leading particle inside the cone $R = \sqrt{\Delta\eta^2 + \Delta\phi^2} = 0.7$, where η and ϕ are the pseudorapidity and the azimuthal angle respectively. Note that the estimated event rate in the CMS acceptance, $\sim 10^7$ jets with $E_T > 100$ GeV in a one month LHC run with lead beams [6,31], will be large enough to carefully study the energy-energy correlations over the whole azimuthal range.

We restrict ourself to central collisions in which the effect of jet quenching is maximum and take into consideration the energy deposition resulting from jets only. The fact is that in the CMS heavy ion physics program the modified sliding window-type jet finding algorithm has been developed to search for "jet-like" clusters above the average energy and to subtract the background from the underlying event [6,31,34]. This developed algorithm allows one to reconstruct the jet energy and its space position with a high enough accuracy in a high multiplicity environment beginning from some threshold jet transverse energy $E_T^{\text{jet}} \sim 50$–100 GeV. Thus, for instance, the reconstruction efficiency (the ratio of the number of reconstructed jets to the total number of generated jets) for jets with energy $E_T^{\text{jet}} > 100$ GeV is close to 100%, the fraction of false jets being not greater than 1% of the total number of reconstructed jets. The mean reconstructed jet energy $E_T^{\text{jet}}(\text{reco})$ is a linear function of the mean generated jet energy $E_T^{\text{jet}}(\text{MC})$, the shape of this dependence being identical in the presence and in the absence of the background from Pb+Pb events. This means that pp-collisions can be used for an adequate comparison with Pb+Pb collisions. The attainable precision of the space resolution of jets is rather high: it is less than the size of a hadron calorimeter tower [6,31,34].

This gives grounds to hope that in the region of maximum energy deposition the contributions from jets and "thermal" background can be effectively separated not only on the simulation level, when they are known *a priori*. Therefore in order to reveal the new possible issues of the investigation of energy correlations we neglect this possible difference between the initially generated and reconstructed jet energy depositions, which can be significant on the outlying jet area only. Though the analysis of the quality of extracting the jet-like energy-energy correlator against background fluctuations based on the detailed simulation of detector responses (together with the optimization of the jet detection threshold and the calibration coefficients used at the subtraction and reconstruction procedures) should be performed for each specific experiment. In particular, in CMS we have to take into consideration that most of the charged low-p_T particles will be cleared out of the central calorimeters by the strong magnetic field (decreasing a really measurable energy flux and absolute value of its fluctuations in such a way).

The results of the numerical simulations are presented in Fig. 2 (for the cases without and with partonic energy loss) for the events containing at least one hard jet with $E_T^{\text{jet}} > E_T(\text{threshold}) = 100$ GeV. The two parametrizations
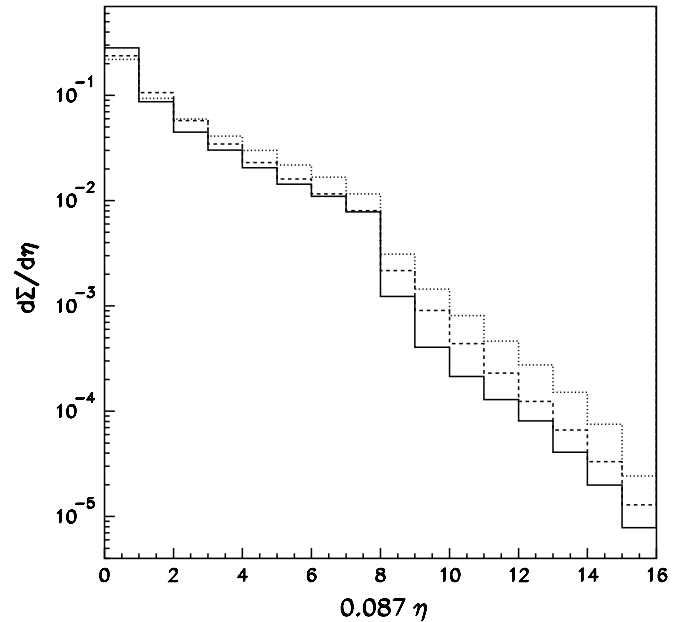

FIG. 2. The transverse energy-energy correlator $d\Sigma_T/d\eta$ in the near-side jet region as a function of pseudorapidity η without (solid histogram) and with medium-induced partonic energy loss for the "small-angular" (7) (dashed histogram) and the "broad-angular" (8) (dotted histogram) parametrizations of emitted gluon spectrum in central Pb+Pb collisions for a jet axis position from the central pseudorapidity region $|\eta^{\text{jet}}| < 0.8$.

of the distribution on the gluon emission angles (7) and (8) were used and $\Delta\eta = \Delta\phi = \Delta\varphi = 0.087$, $M = 8$. One can see that the energy loss results in the noticeable broadening of jet shape which can be characterized by the variation of the mean pseudorapidity squared (the width of distribution). These mean values of pseudorapidity squared are defined in the following form:

$$\langle \eta^2 \rangle = \int d\eta \, \eta^2 \frac{d\Sigma_T(\eta)}{d\eta} \bigg/ \int d\eta \frac{d\Sigma_T(\eta)}{d\eta} \quad (9)$$

and are displayed in Table I. They are mainly determined by the first bins of histograms closed to a jet axis where the separation of jet and background contributions to the total energy deposition is expected to be effective. The broadening effect is considerable for the "broad-angular" radiation, comes to $\sim 45\%$ and probably can be observable in spite of the ambiguities discussed above.

Figure 3 shows the behavior of correlator (6) in the near-side jet region as a function of azimuthal angle φ (the notations and the kinematical restrictions are the same as in Fig. 2). As in the previous case the broadening is more pronounced for the "broad-angular" parametrization of emitted gluon spectrum. Besides the equality (with a good accuracy) of mean values of pseudorapidity and azimuthal angle squared results from the rapidity-angle symmetry of jet shape for jets from the central pseudorapidity region. For the illustration the difference between correlators

$$\left(\frac{d\Sigma_T(\eta)}{d\eta} - \frac{d\Sigma_T(\varphi)}{d\varphi} \right)\bigg|_{\eta=\varphi}$$

TABLE I. The mean values of pseudorapidity and angle squared as a measure of the width of transverse energy-energy correlation functions.

Model	Without loss	Energy loss (7) off comoving constituents	Energy loss (8) off comoving constituents	Energy loss (7) off "slow" constituents	Energy loss (8) off "slow" constituents
			$|\eta^{\text{jet}}| < 0.8$		
$\langle \eta^2 \rangle$	0.029	0.033	0.042	0.034	0.051
$\langle \varphi^2 \rangle$	0.030	0.034	0.044	0.035	0.054
			$0.8 < \eta^{\text{jet}} < 2.4$		
$\langle \eta^2 \rangle$	0.028	0.032	0.044	0.046	0.055
$\langle \varphi^2 \rangle$	0.028	0.033	0.045	0.048	0.056

as a function of $\eta = \varphi$ is presented in Fig. 4. This difference is small, nonregular and comes to the level of statistical fluctuations.

We are interested in the nonsymmetrical behavior of correlators as functions of pseudorapidity and azimuthal angle because there is some discussion in the current literature [9] about the possible nonsymmetrical modification of jet shape due to the collective motion of medium constituents, on which the rescattering of jet partons takes place. The correlators under consideration could show the different behavior over angle and pseudorapidity for a jet axis position from the nonsymmetrical pseudorapidity region. However our simulation gives practically the former results for correlators calculated for jets from the noncentral pseudorapidity region $0.8 < \eta^{\text{jet}} < 2.4$. The corresponding values of pseudorapidity

and angle squared are listed in the lower part of Table I. The difference between correlators as a function of $\eta = \varphi$ is again small, nonregular and comes to the level of statistical fluctuations as in Fig. 4.

Thus the behavior of transverse energy-energy correlators in the near-side jet region is independent of the pseudorapidity position of a jet axis. The fact is that in our model the rescattering of a hard parton takes place off a comoving medium constituent (i.e., moving with the same longitudinal rapidity as a hard parton). In such approach gluons are emitted at the polar angle θ relative to the *transverse momentum* p_T of a radiating parton isotropically over the azimuthal angle in the rest frame of a medium constituent that, as a matter of fact, provides for the longitudinal boost invariance of correlators. However this scenario with the same longitudinal rapidity of a
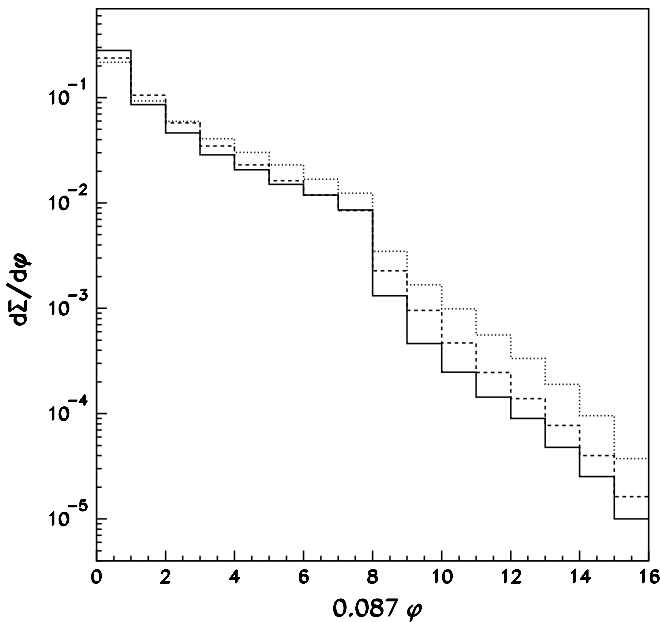

FIG. 3. The transverse energy-energy correlator $d\Sigma_T/d\varphi$ in the near-side jet region as a function of azimuthal angle φ without (solid histogram) and with medium-induced partonic energy loss for the "small-angular" (7) (dashed histogram) and the "broad-angular" (8) (dotted histogram) parametrizations of emitted gluon spectrum in central Pb+Pb collisions for a jet axis position from the central pseudorapidity region $|\eta^{\text{jet}}| < 0.8$.
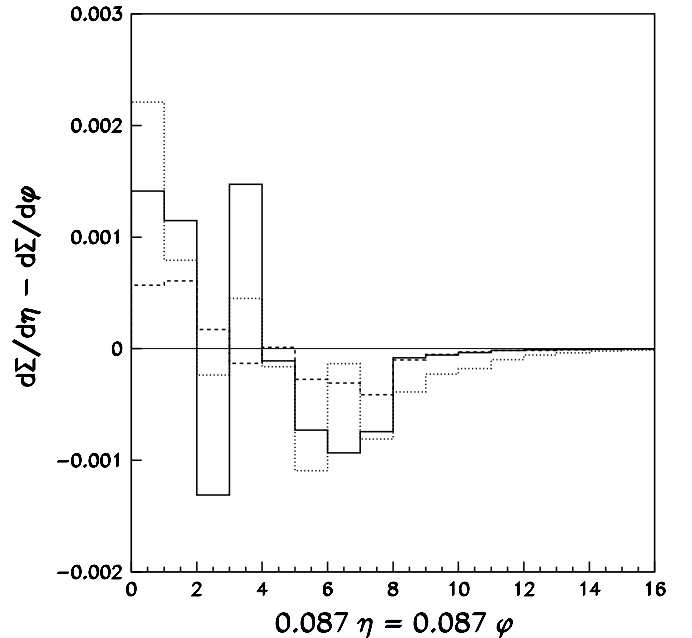

FIG. 4. The difference between correlators $(\frac{d\Sigma_T(\eta)}{d\eta} - \frac{d\Sigma_T(\varphi)}{d\varphi})|_{\eta=\varphi}$ in the near-side jet region as a function of $\eta = \varphi$ without (solid histogram) and with medium-induced partonic energy loss for the "small-angular" (7) (dashed histogram) and the "broad-angular" (8) (dotted histogram) parametrizations of emitted gluon spectrum in central Pb+Pb collisions for a jet axis position from the central pseudorapidity region $|\eta^{\text{jet}}| < 0.8$.

jet parton and a medium constituent (mostly used and closely related with the Bjorken scaling solution) is not unique and one can suppose that a jet parton and a medium constituent move in the longitudinal direction in a different way.

On the generator level it is not difficult to realize the scenario when the rescattering takes place off a so-called "slow" medium constituent (i.e., moving with the zero or considerably less longitudinal rapidity in comparison with the rapidity of a jet parton) and gluons are emitted at the polar angle θ relative to the *total momentum p* of a parent parton. From Table I one can see that for jets from the central pseudorapidity region $|\eta^{\text{jet}}| < 0.8$ and the "small-angular" parametrization (7) this modification does not lead to any variation of correlation functions because of the small distinction between the total and transverse momenta in this case. For the "broad-angular" radiation (8) the broadening of jet shape is independent of the rescattering scenario in the central pseudorapidity region at the additional restriction on the difference between the directions of an initial hard parton and a final jet axis (due to the large "tail" in the distribution over this difference).

For jets from the forward pseudorapidity region $0.8 < \eta^{\text{jet}} < 2.4$ (where the distinction between the total and transverse momenta is significant) the broadening of jet shape increases considerably that is supported by the calculated mean values of pseudorapidity and angle squared. This larger broadening results from that the energy loss is determined by not the transverse momentum (as this was early) but the total one which is considerably larger than the transverse momentum for jets from the forward pseudorapidity region. The experimental observation of such dependence of the width of correlation functions on the pseudorapidity position of a jet axis will indicate the scenario with the gluon radiation around the total momentum of a parent parton. Besides this observation does not demand the comparison with *pp*-collisions, in which such dependence is absent.

As regards the possible $\eta \times \varphi$ asymmetry, then it is invisible as before on the level of the mean values, although we might catch some regular (but again practically on the level of statistical fluctuations) difference in the behavior of correlators over η and φ. This can mean that the transverse energy-energy correlations (unlike the average jet energy and jet multiplicity [9]) is weakly sensitive to longitudinal flow effects due to the longitudinal Lorentz invariance of transverse energy itself or our simple imitation of flow effects on the generator level can be, in principle, not enough to their study in respect of the possible $\eta \times \varphi$ asymmetry.

The scenarios suggested above result also in the different dependence of jet quenching on the pseudorapidity. In the accepted scenario (I) with the rescattering off comoving medium constituents jet quenching is expected to be independent of the jet pseudorapidity under the condition that the matter density is also η-independent and Fig. 5 demonstrates this independence. We define a jet quenching factor R in a conventional way,

$$R = \frac{N(E_{\text{jet}} > 100 \text{ GeV})|_{\text{with losses}}}{N(E_{\text{jet}} > 100 \text{ GeV})|_{\text{without losses}}}, \quad (10)$$

as the ratio of the jet number with transverse energy $E_T^{\text{jet}} > 100$ GeV with energy loss to the corresponding number of
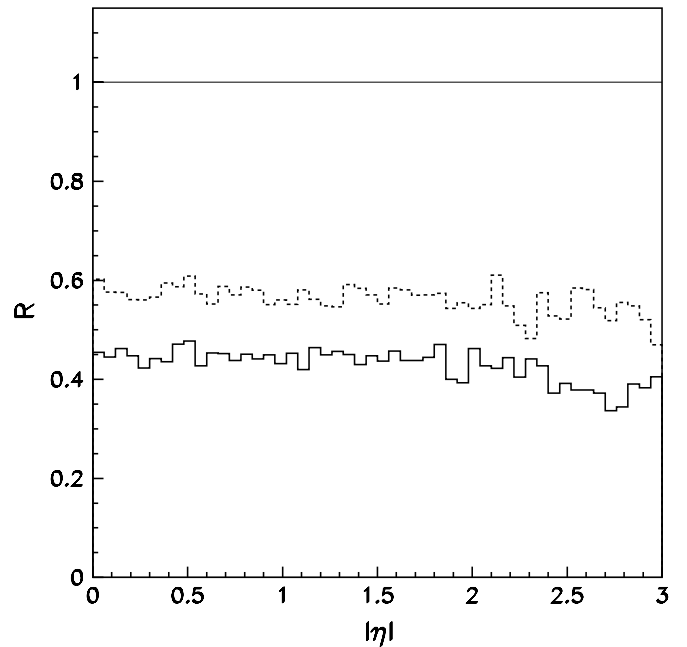

FIG. 5. The jet quenching factor R as a function of pseudorapidity η without (solid line) and with medium-induced partonic energy loss for the "small-angular" (7) (dashed histogram) and the "broad-angular" (8) (solid histogram) parametrizations of emitted gluon spectrum in central Pb+Pb collisions in scenario I.

jets without loss (i.e., in *pp*-collisions normalized on the number of binary nucleon-nucleon sub-collisions). In the second scenario (II) a quenching factor is strongly (Fig. 6)
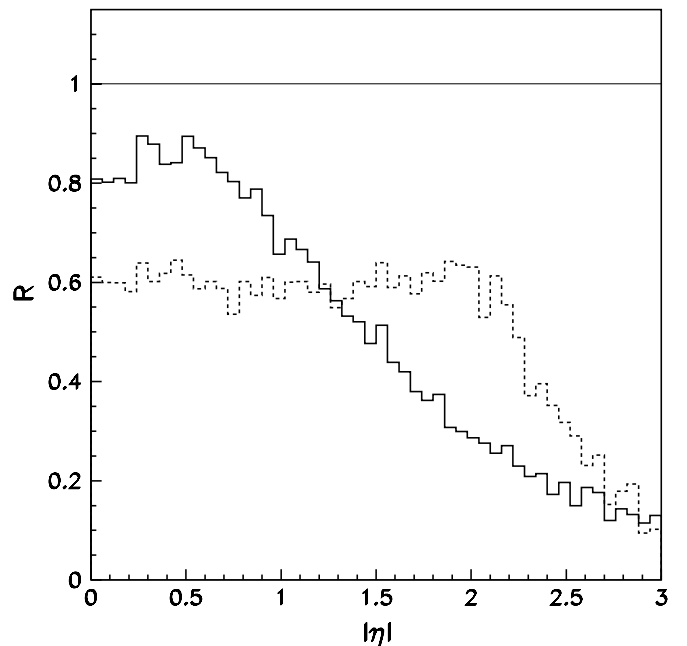

FIG. 6. The jet quenching factor R as a function of pseudorapidity η without (solid line) and with medium-induced partonic energy loss for the "small-angular" (7) (dashed histogram) and the "broad-angular" (8) (solid histogram) parametrizations of emitted gluon spectrum in central Pb+Pb collisions in scenario II.
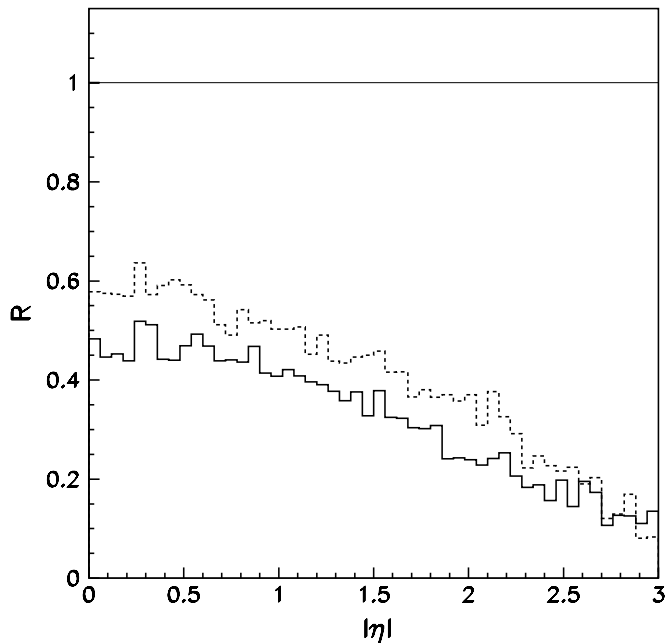
FIG. 7. The jet quenching factor R as a function of pseudorapidity η without (solid line) and with medium-induced partonic energy loss for the "small-angular" (7) (dashed histogram) and the "broad-angular" (8) (solid histogram) parametrizations of emitted gluon spectrum in central Pb+Pb collisions in scenario II under the additional restriction on the difference between the directions of an initial hard parton and a final jet axis (<0.2).

dependent on the pseudorapidity position of a jet axis. For the "broad-angular" radiation this factor R has more tangled behavior with the shifted (not in the zero) maximum over η. This can be explained by the large "tail" in the distribution over the difference (especially in $\eta \times \varphi$ space) between the directions of an initial hard parton and a final jet axis and by our simplified jet definition. Here the final jet energy is defined simply as the total transverse energy of final particles collected around the direction of a leading particle inside the cone $R = \sqrt{\Delta\eta^2 + \Delta\phi^2} = 0.7$ without correction of the jet axis usually used in the modified sliding window-type jet finding algorithm. The structure with the pseudorapidity-shifted

maximum disappears if the restriction on the difference between the directions of an initial hard parton and a final jet axis is established as one can see in Fig. 7 or if the modified sliding window-type jet finding algorithm [6,31,34] is used. But for all that the additional restriction and the use of other algorithm have no influence on the rapidity-behavior of quenching factor in the scenario I. Thus the quenching factor together with the jet shape broadening is independent of the pseudorapidity position of a jet axis in the scenario I while in the scenario II the dependence of these observables on the pseudorapidity is noticeable and probably can be experimentally detected in spite of ambiguities discussed above.

V. SUMMARY

The special correlator in the vicinity of maximum energy deposition of every event allowed us to investigate the jet shape modification due to partonic energy loss using the calorimetric information. In the accepted scenario with scattering of jet hard partons off comoving medium constituents this correlator is independent of the pseudorapidity position of a jet axis and becomes considerably broader (symmetrically over the pseudorapidity and the azimuthal angle) in comparison with pp-collisions. At scattering off "slow" medium constituents the broadening of correlation functions is dependent on the pseudorapidity position of a jet axis and increases noticeably in comparison with the previous scenario for jets with large enough pseudorapidities. These two considered scenarios result also in the different dependence of jet quenching on the pseudorapidity. We believe that such a transverse energy-energy correlation analysis may be useful at LHC data processing.

[1] M. C. Abreu *et al.* (NA50 Collaboration), Phys. Lett. **B410**, 337 (1997); B. Alessaudro *et al.* (NA50 Collaboration), Eur. Phys. J. C **39**, 335 (2005).

[2] G. Agakichiev *et al.* (CERES Collaboration), Phys. Rev. Lett. **75**, 1272 (1995).

[3] U. W. Heinz and M. Jacob, nucl-th/0002042 (2000).

[4] H. Satz, Nucl. Phys. **A715**, 3 (2003).

[5] P. Jacobs and X.-N. Wang, Prog. Part. Nucl. Phys. **54**, 443 (2005).

[6] A. Accardi *et al.*, Jet physics, in Hard probes in Heavy Ion Collisions at the LHC, edited by M. Mangano, H. Satz, and U. Wiedemann, CERN Report 2004-09 (2004), hep-ph/0310274.

[7] J. Pan and C. Gale, Phys. Rev. D **50**, 3235 (1994).

[8] I. P. Lokhtin, L. I. Sarycheva, and A. M. Snigirev, Eur. Phys. J. C **36**, 375 (2004).

[9] C. A. Salgado and U. A. Wiedemann, Phys. Rev. Lett. **93**, 042301 (2004); N. Armesto, C. A. Salgado, and U. A. Wiedemann, *ibid.* **93**, 242301 (2004); Phys. Rev. C **72**, 064910 (2005).

[10] P. Abreu *et al.* (DELPHI Collaboration), Phys. Lett. **B252**, 149 (1990); Z. Phys. C **59**, 21 (1993); M. Akrawy *et al.* (OPAL Collaboration), Phys. Lett. **B252**, 159 (1990); **B276**, 547 (1992); B. Adeva *et al.* (L3 Collaboration), *ibid.* **B257**, 469 (1991); O. Adriani *et al.* (L3 Collaboration), *ibid.* **B284**, 471 (1992).

[11] K. Abe *et al.* (SLD Collaboration), Phys. Rev. D **50**, 5580 (1994); **51**, 962 (1995).

[12] C. L. Basham, L. S. Brown, S. D. Ellis, and S. T. Love, Phys. Rev. Lett. **41**, 1585 (1978); Phys. Rev. D **17**, 2298 (1978).

[13] A. Ali, E. Pietarinen, and W. J. Stirling, Phys. Lett. **B141**, 447 (1984).

[14] N. A. Kruglov, I. P. Lokhtin, L. I. Sarycheva, and A. M. Snigirev, Z. Phys. C **76**, 99 (1997).

[15] I. P. Lokhtin and A. M. Snigirev, Eur. Phys. J. C **16**, 527 (2000).

[16] I. P. Lokhtin, L. I. Sarycheva, and A. M. Snigirev, Phys. Atom. Nucl. **62**, 1258 (1999).

[17] S. A. Bass *et al.*, Nucl. Phys. **A661**, 205c (1999).

[18] I. P. Lokhtin and A. M. Snigirev, Phys. Lett. **B440**, 163 (1998).

[19] I. P. Lokhtin, S. V. Petrushanko, L. I. Sarycheva, and A. M. Snigirev, Phys. At. Nucl. **65**, 943 (2002).

[20] I. P. Lokhtin, S. V. Petrushanko, L. I. Sarycheva, and A. M. Snigirev, CERN CMS Note 2003/019 (2003).

[21] I. P. Lokhtin, L. I. Sarycheva, and A. M. Snigirev, Phys. Lett. **B537**, 261 (2002); Nucl. Phys. **A715**, 633c (2003).

[22] I. P. Lokhtin, L. I. Sarycheva, and A. M. Snigirev, Eur. Phys. J. C **30**, 103 (2003).

[23] I. P. Lokhtin and A. M. Snigirev, Phys. Lett. **B567**, 39 (2003).

[24] I. P. Lokhtin and A. M. Snigirev, Eur. Phys. J. C **45**, 211 (2006).

[25] I. P. Lokhtin, http://cern.ch/lokhtin/pyquen.

[26] T. Sjostrand, Comput. Phys. Commun. **135**, 238 (2001).

[27] R. Baier, Yu. L. Dokshitzer, A. H. Mueller, and D. Schiff, Phys. Rev. C **60**, 064902 (1999); **64**, 057902 (2001).

[28] B. G. Zakharov, JETP Lett. **70**, 176 (1999).

[29] U. A. Wiedemann and M. Gyulassy, Nucl. Phys. **B560**, 345 (1999); U. A. Wiedemann, *ibid.* **B588**, 303 (2000); **A690**, 731 (2001).

[30] M. Gyulassy, P. Levai, and I. Vitev, Nucl. Phys. **B571**, 197 (2000); Phys. Rev. Lett. **85**, 5535 (2000); Nucl. Phys. **B594**, 371 (2001).

[31] G. Baur *et al.*, Heavy Ion Physics Programme in CMS, CERN CMS Note 2000/060 (2000).

[32] J. D. Bjorken, Phys. Rev. D **27**, 140 (1983).

[33] K. J. Eskola, K. Kajantie, and K. Tuominen, Phys. Lett. **B497**, 39 (2001); K. J. Eskola, P. V. Ruuskanen, S. S. Rasanen, and K. Tuominen, Nucl. Phys. **A696**, 715 (2001).

[34] I. N. Vardanian, I. P. Lokhtin, L. I. Sarycheva, A. M. Snigirev, and C. Y. Teplov, Phys. At. Nucl. **68**, 332 (2005).